CRACK ANALYSIS OF CLADDED MOCKUPS IN THE FRAME OF BRITTLE FRACTURE.

Gilles DEBRUYNE*, Dominique MOINEREAU**.

Results of experimental tests and 3D numerical analysis are presented for three bending loaded cladded mockups with different undercladding or ermerging defects. The numerical prediction of the crack initiation loading is in a good agreement with the experimental results. Comparisons between present numerical study and analyzes without modelling cladding show the reducing effect of the cladding on the energy release rate. In most of the cases, 2D analyzes are too much conservative.

INTRODUCTION.

To prove innocuity of flaws in PWR vessel, particularly at the end-of-life because of the radiation embrittlement of the vessel material , EDF has engaged a programme including both experimental tests on large size mockups and numerical analyses. The objective of our communication is to present 3D numerical results for different cracked mockups configurations, to compare them with experimental results and to show the favourable effect of cladding.

EXPERIMENTAL PROGRAMME.

Large size mockups, containing artificial defects, are submitted to mechanical tests.The mockup chosen to simulate the vessel is a four-point bend bar specimen shown schematically in figure 1.
The material of central part of each mockup is A508 Cl3 ferritic steel. The mockups of approximately 120 mm thickness, 1700 mm length and 150 mm width are layered on top surface with stainless steel, and they receive a stress relief heat treatment. Each mockup contains an artificial defect made by machining and fatigue.

* ELECTRICITE DE FRANCE, SERVICE IMA, CLAMART, FRANCE.
** ELECTRICITE DE FRANCE, SERVICE RNE, LES RENARDIERES, FRANCE.

Many configurations are tested in the programme.We analyze here three configurations :

-specimen DSR4 containing small underclad semi-elliptical crack in the Heat Affected Zone of the base metal, of 5 mm depth and 50 mm width, with a cladding of 7.5 mm thickness.

- specimen DSR3 with underclad semi-elliptical crack of 13 mm depth and 39 mm width, with a cladding of 4.5 mm thickness.

-specimen DD1' with an emerging through clad thickness semi-circular crack of 34 mm depth.

The mockups are loaded in four-point bending (cf. fig. 1) until crack instability by cleavage fracture. Testings are performed at very low temperature to obtain a cleavage fracture toughness K_{Ic} of the base metal representative of the vessel material toughness at the end of the lifetime. Cooling is obtained with liquid nitrogen and during testing, the specimen is insulated to avoid reheating. Data collected during tests are: load, load-point displacement, crack-mouth opening displacement in case of emerging crack, and strains measured with strain gages placed on the top (cladding) and bottom surfaces. Thermocouples are placed on surface and inside the specimens to determine the temperature during the test. The fracture toughness is measured on small CT 25 specimens (20% side-groved) .

MECHANICAL ANALYSES.

Each test is interpretated with linear elastic analysis, elastic-plastic analysis and local approach of fracture [1]. For each configuration presented above, we point out in this paper the 3D numerical results obtained with linear elastic analysis and with non linear analysis (HENCKY law).

Modelization of the mockups.

We use 3D F.E.M. to analyze each test. Taking account of symmetries, only a quarter of specimen is meshed as shown in figure 3. The mesh is composed with 20 nodes bricks and 15 nodes wedges. In spite of the sharpness of this mesh all around the crack front, the larger model has less of 800 elements and 3000 nodes. For the elastic-plastic calculation, we assume that the Deformation Theory of Plasticity is valid [2] for this kind of structure. For each calculation, we use the general finite element code PERMAS [3] on a CRAY YMP.

The energy release rate formulation using the theta method.

To perform fracture analysis, SIF (stress intensity factors)

K_I and K_J are calculated all along the crack front. The criterion of instability by cleavage fracture is the classical: K_I(or K_J) = K_{Ic}, where K_{Ic} is the material toughness. In fact, we calculate the energy release rate G, using a Lagrangian method called THETA method which leads to an exact derivative of the potential energy W with respect of the domain variation. This method, introduced by DESTUYNDER [4] , consists, in a virtual cinematic of the crack (modelized by a vector field θ within the domain Ω of the structure), to solve the elastic problem (linear or non linear) in the Lagrangian configuration.
The expression of G is:

$$G(\theta) = \int_\Omega [-\omega(\epsilon) div\theta + \sigma : (\nabla u \nabla \theta)] \, d\Omega ,$$

where $\omega(\epsilon)$ is the elastic potential, σ and ϵ the stress and the strain field, u the displacement field. The quantity $G(\theta)$ depends only on the θ field values on the crack front. This method was already used with success for 3D non linear elastic law by Y.WADIER [5].

NUMERICAL RESULTS AND INTERPRETATION OF TESTS.

DSR3 mockup.

This mockup has a semi-elliptical flaw with size 13 mm depth and 39 mm width. The crack instability by cleavage is reached with a load of 695 KN at a temperature of about -170°C. We used a non linear law in calculus in spite of the brittle fracture of the mockup, because stresses in the cladding are very high (MISES stresses are beyond the yield strength of the stainless steel at -170°C, which is about 350 MPa), while the stresses in the ferritic steel never exceed the yield strength (about 750 MPa). The maximum of SIF in the base metal, at the tip of the crack is 53 MPa $\sqrt{m}$, which is in the scatter band of material toughness (between 40 and 55 MPa $\sqrt{m}$ at the test temperature). The measured strains (gages J1 to J6 on the top of the cladding cf fig 2 and J7-J8 on the face in compression) are compared to the computed strains in the table 1.We also calculated the same mockup, suppressing the cladding whose mechanical effect is neglected in the American rules. Three SIF curves along the crack front (with respect to the parametric angle),are drawn in the figure 3. They represent the non-linear and the linear calculus, taking account of cladding, and a linear calculus where cladding is suppressed. We can notice the favourable effect of cladding on the SIF values, which decrease. Of course, K_J at the interface base metal-cladding is very high (the maximum value is about 82 MPa $\sqrt{m}$) but the toughness of stainless steel is more than 100 MPa $\sqrt{m}$, so that the failure occurs without ductile fracture. In the other hand, as we can see in figure 3, comparing the results of the non-linear and the linear calculus, the plasticity in the cladding make SIF(with no plastic correction) higher along the crack front.

Gauges position	ϵ_{zz} measure (10^{-6})	ϵ_{zz} computed
J1	2692	2420
J2	2582	2800
J3	3679	3900
J4	3080	2800
J5	2617	2420
J6	2324	1660
J7	2480	1880
J8	-2016	-2400
J9	-2024	-2400

TABLE 1: Comparisons between measures and computation of strains.

DSR4 mockup.

This mockup has a semi-elliptical flaw with size 5 mm depth and 50 mm width. The crack instability by cleavage is reached with a load of 640 KN at a temperature of about -170°C, -180°C. For this load, we find a maximum SIF, at the crack tip, of 50 MPa$\sqrt{m}$ after a non-linear calculation (a linear modelization leads to K_I= 41 MPa$\sqrt{m}$)

2D modelizations do not lead to very different results because the flaw is nearly a strip crack. The SIF values are in the band of toughness. Figure 4 shows the SIF values along the crack front with and without the cladding. This latter has a dropping effect on the SIF values.

DD1' mockup.

For this mockup, a quasi semi-circular crack of 34 mm depth is emerging through the cladding. The collapse load is 357 KN at a temperature of about -170, -180°C. For this load, we find a maximum SIF of 51 MPa$\sqrt{m}$ near the free surface (with a linear model because no plasticity occurs). This result is in a good agreement with formula of J.C. NEWMAN and I.S. RAJU [6] for bending loads (for the same geometry, this formula lead to K_I= 48 MPa$\sqrt{m}$). We can notice in the figure 5 that, contrary to the two above mockups, the SIF value increases from tip to emerging surface crack. Of course, just at the free surface the SIF value must be equal to zero, but it decreases in a short boundary layer that we cannot discerne with classical finite elements.

Residual stresses.

Some measures of residual stresses have been carried out by MPA Stuttgart with two different techniques (layering technique and ring core method). The figure 6 shows the longitudinal and transversal stresses in the cladding (from 200 to 300 MPa) and in

the base metal (about -50 MPa). These values are confirmed by simple 2D thermoplastic analysis simulating the heat treatment. The zone of the located defect is not very affected by those stresses (between -50 and 50 MPa).

CONCLUSION.

The main conclusions we can draw from this study are :

- The nature of fracture, for the base metal, is cleavage for every test, for conditions simulating end-of-life vessel, even if the cladding can be plastified.

- The prediction of fracture by 3D non linear analysis is correct despite of the residual stresses in cladding, which are not included in our models but are not so important.

- The conservatism of analysis neglecting the cladding is too much strong (for the critical load, the SIF is then outside the band of toughness).

At this time, other tests are in progress with new configurations. We will have to consider some theorical problems about singularity of stresses at the interface of two different materials, which are not yet solved.

REFERENCES

[1] D. MOINEREAU, M. BETHMONT, G. DEBRUYNE, G. ROUSSELIER (1990): Brittle fracture behaviour of cracks in reactor pressure vessel EDF programme's presentation. First testings and interpretation by fracture mechanics - Pressure Vessel Piping Conference, Nashville.

[2] Y. WADIER (1987): Analysis of a compact tension specimen in 3D elastoplastic fracture mechanics. Finite Element in Engineering Applications - INTES- Stuttgart.

[3] E.SCHREM, K. BERNHARD, H. KNAPP (1985) : PERMAS part I. Linear static analysis User's Reference Manual. INTES Pub. N 202, rev.H

[4] Ph. DESTUYNDER, M. DJAOUA (1980): Equivalence de l'intégrale de Rice et du taux de restitution d'énergie- C.R. Acad. Sc. Paris.

[5] Y. WADIER, O. MALAK (1989): The Theta Method Applied to the Analysis of 3D Elastic-Plastic Cracked Bodies - SMIRT 10 Anaheim.

[6] J.C. NEWMAN, IS. RAJU (1981): An empirical stress-intensity factor equation for the surface crack - Engineering Fracture Mechanics, Vol. 15, N° 1-2,pp. 185-192.

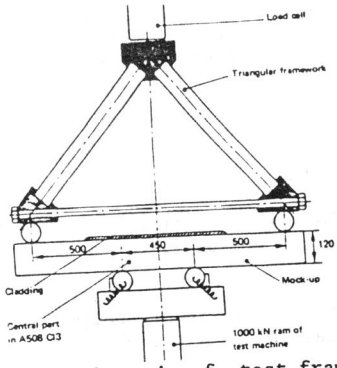

Fig.1 Schematic of test frame

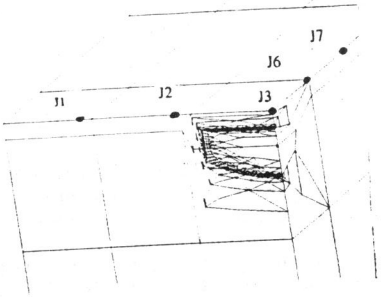

Fig.2 Mesh of DSR3 mockup.

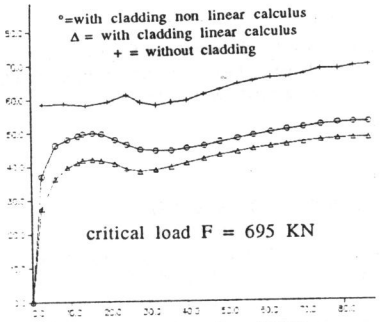

Fig.3 SIF curves for DSR3

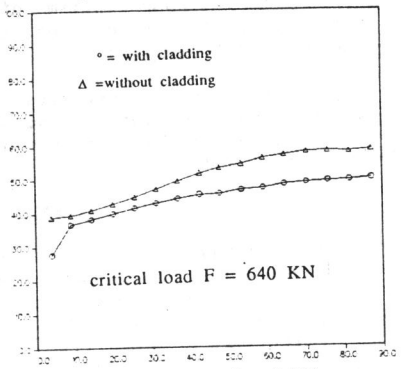

Fig. 4 SIF curves for DSR4

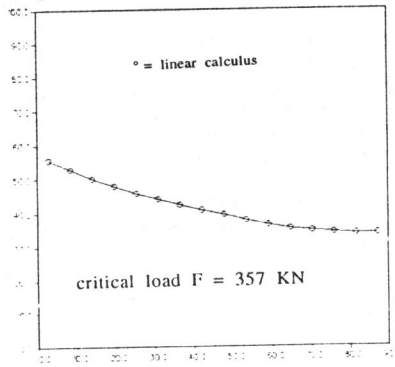

Fig.5 SIF curves for DD1'

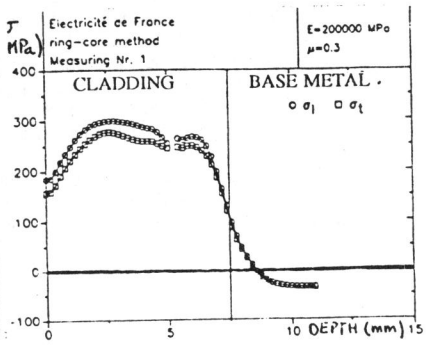

Fig.6 Residual stresses measures